Development of a Two Link Robotic Manipulator

OLAOLUWA D. ALADETOLA[1], KAYODE F. AKINGBADE[2], NAJEEM O. ADELAKUN[3]
[1, 3] *Department of Electrical and Electronics Engineering, Federal Polytechnic Ilaro, Ogun State.*
[2] *Department of Electrical and Electronics Engineering, Federal University of Technology, Akure, Ondo State.*

Abstract- Robots play important roles in day to day activities of human endeavour and can perform complex tasks speedily and accurately. Robots are employed to imitate human behaviours and then apply these behaviours to the skills that lead to achieving a certain task in solving the challenges faced by impaired people in society. This robotic arm was achieved using light-weight steel iron for the frames, a moderate torque MG995 Towerpro, and servo motor. Two Atmega328 Arduino microcontroller was employed to control the motors through the use of pulse width modulation technique. Mathematical models were developed for the mechanism to represent the kinematics involved at each joint with mathematical variables. Then, the stability of the system was carried out using a step input signal being a type zero system.

Indexed Terms- Robot, armature dc servo motors, Arduino microcontroller, stability.

I. INTRODUCTION

The rapid growth in technology prompt for the latest matching devices. However, engineers and scientists are vastly adapting new technologies persistently. The robots perform significant roles in our lives and can carry out complex responsibility faster and accurately when compared to humans. They do not get drained or perform task emotionally. Robots operate in almost all human labours mostly in the fields which are unhealthy or impractical for workers [3]. This fact causes the workers to have more free time to spend on skilled Professions which includes the programming, maintenance, and operation of the robots.

Robotic arms perform simple translational and rotational motion, which has an end effector that performs a specific function [4]. A Robot is a programmable mechanical device that can replace the functions of the human arm. An automated pick and place robot arm, which can reach an object in a given domain or range of space, grip it precisely, and place it to the desired position. This mechanism is used for lifting objects and carrying out tasks that require extreme concentration, expert accuracy and may also be recursive. It can be employed industrially (e.g. cranes). According to [12] Presently industrial arms have risen in its capability and operation through micro-controllers and programming developments, enhanced mechanisms, sensing, and drive systems, which has led to a vast transformation in the robotic industry [4]. Hence, when designing a robot, factors such as artificial intelligence, concept and techniques, and cognitive science are vital to obtaining a viable design.

II. SYSTEM MODELLING

System modelling involves the use of models to conceptualize and construct real-life to analyse, study and simulate the real-life situations or system virtually. This gives us deeper insight into other aspects of the system and this helps in determining the stability and other characteristics of the system. Figure 1 shows that the model has a base upon which other parts of the manipulator is placed upon. Directly on the base is the shoulder link, this link is expected to undergo two different motion patterns first in the 180^0 rotation of the base giving the mechanism the aid to pick and place any desired target within its circumference of operation [5]. In addition to this motion, another actuator will be used to perform a translational motion at an angle which is used to move the next link, the elbow. At the joint between the shoulder and the elbow, another actuator is used making the third that helps to move the elbow link at an angle translational. Thereafter the end-effector is put in place to perform the picking and placing of the target object. The motion of the end-effector is also done with the aid of actuators and gears [6]. This gives a brief overview of the whole mechanism and how the links are connected one to another.

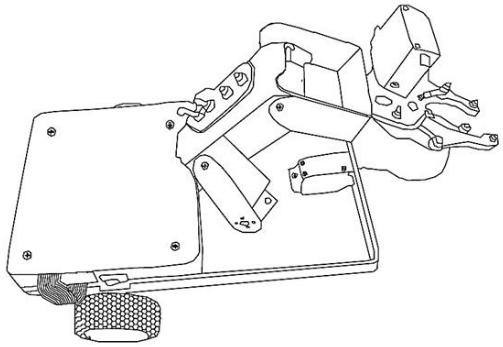

Fig. 1. Two link robotic manipulator system

III. MATHEMATICAL MODELLING OF THE SYSTEM

The Rotational Double Inverted Pendulum (RDIP) described here consists of a horizontal base arm (denoted as Link 1) driven by a servo motor and two vertical pendulums. The mathematical model of the RDIP was developed by the use of the Euler-Lagrange (E-L) function [8].

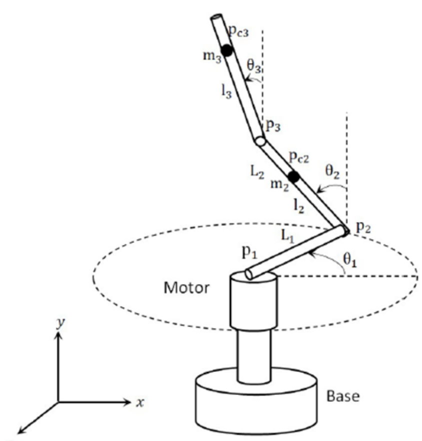

Fig. 2. Rotational double inverted pendulum schematic [11].

Θ_1 is the angle of link 1in the horizontal plane
$\dot{\theta}_1$ is the velocity of link 1in the horizontal plane
$\ddot{\theta}_1$ is the acceleration of link 1
Θ_2 is the angle of link 2 in the vertical plane
$\dot{\theta}_2$ is the velocity of link 2 in the vertical plane
$\ddot{\theta}_2$ is the acceleration of link 2
Θ_3 is the angle of link 3 in the horizontal plane
$\dot{\theta}_3$ is the velocity of link 3 in the horizontal plane
$\ddot{\theta}_3$ is the acceleration of link 3
J_1 is the moment of inertial for link 1

The equation of motion for the system dynamic is expressed from the Fig.3

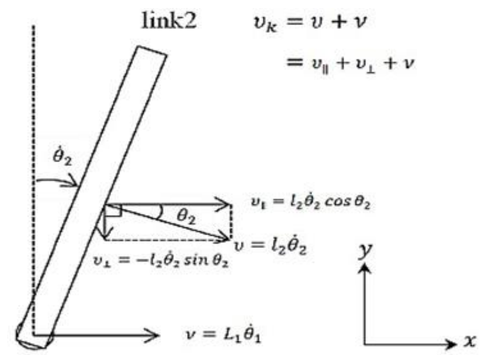

Fig. 3. Velocity analysis for link 2

The total kinetic energy of each link in our system is given by the combination of its moving kinetic term K_m and its rotating kinetic term K_r as

$$K_m=\frac{1}{2}mv^2$$
$$K_r=\frac{1}{2}j\dot{\theta}_i^2 \quad (1)$$

From Fig.3 the total kinetic energy for both links is expressed as

$$k=\frac{1}{2}j\dot{\theta}_i^2+\frac{1}{2}j\dot{\theta}_2^2+\frac{1}{2}j\dot{\theta}_3^2+\frac{1}{2}m_2[(L_1\dot{\theta}_1+i_2\dot{\theta}_2\sin\theta_2)^2+(-i_2\dot{\theta}_2\sin\theta_2)^2]+\frac{1}{2}m_3[(L_1\dot{\theta}_1+i_2\dot{\theta}_2\cos\theta_2+i_3\dot{\theta}_3\cos\theta_3)^2+(-i_2\dot{\theta}_2\sin\theta_2-i_3\dot{\theta}_3\sin\theta_3)^2] \quad (2)$$

And the potential energy expressed as

$$P=m_3gl_2\cos\theta_2+m_3g(L_2\cos\theta_2+i_3\cos\theta_3) \quad (3)$$

From langrange function

If $L = K - P$ (4)

Applying eqn (2) and (3) to eqn (4)

$$\frac{d}{dt}\frac{\partial L}{\partial\dot{\theta}_1}-\frac{\partial L}{\partial\theta_1}=\tau-b_1\dot{\theta}_1 \quad (5)$$

Finding the derivatives from eqn (5)

$$\tau=(j_1+L_1^2(m_2+m_3))\ddot{\Theta}_1+l_1(m_2l_2+m_3L_2)\cos\Theta_2\ddot{\Theta}_2+l_1m_3l_3\cos\Theta_3\ddot{\Theta}_3+b_1\dot{\theta}_1L_1(m_2l_2+m_3L_2)\dot{\Theta}^2{}_1\sin\Theta_2-L_1m_3l_3\Theta^2{}_3\sin\Theta_3$$
(6)

$$\frac{d}{dt}\frac{\partial L}{\partial \dot{\theta}_1} - \frac{\partial L}{\partial \theta_2} = \tau - b_2\dot{\theta}_2$$

$$0 = -L_1(m_2 l_2 + m_3 l_2)\cos\theta_2\,\theta_1 - (j_2 + L_2^2 m_3 + l_2^2 m_2)\theta_2 - L_2 m_3 l_3\cos(\theta_2 - \theta_3)\theta_3 - b_2\dot{\theta}_2 - L_2 m_3 l_3 \Theta^2{}_3 \sin(\theta_2 - \Theta_3) + (m_2 l_2 + m_3 L_2) g \sin\theta_2 \quad (7)$$

And

$$\frac{d}{dt}\frac{\partial L}{\partial \dot{\theta}_2} - \frac{\partial L}{\partial \theta_3} = \tau - b_3\dot{\theta}_3 \quad (8)$$

$$0 = -L_2 m_3 l_3 \cos\theta_2\theta_1 - L_2 m_3 l_3 \cos(\theta_2 - \theta_3)\theta_2 - (j_3 + l_2^2 m_3)\theta_3 - b_3\dot{\theta}_3 + L_2 m_3 l_3 \dot{\theta}_3^2 \sin(\theta_2 - \theta_3) + m_3 l_3 g \sin\theta_3. \quad (9)$$

IV. THE FORCE AND TORQUE REQUIRED

The mass of the links and the actuators are both considered in computing the torque at each joint. The length and the mass of various components are highlighted below in Figure 4.

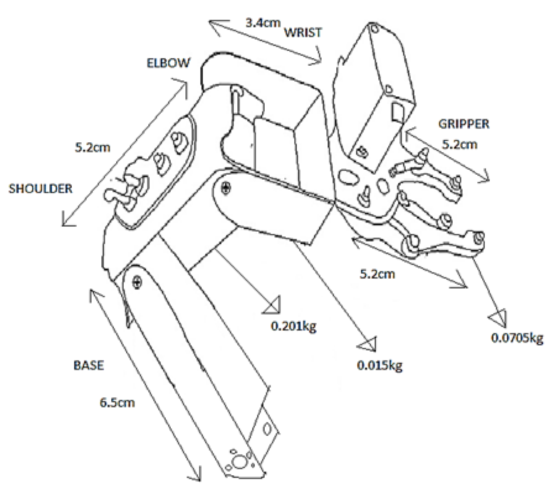

Fig .4. Mass and length of the robotic arm links

Mass of servo meter used = 52g = 0.052kg
Length of the shoulder = 7.2cm,
Mass of the shoulder link = 0.0201kg
Length of the elbow = 10.4cm,
Mass of the elbow link = 0.402kg
Length of the wrist = 3.2cm,
Mass of the wrist link = 0.015kg
Length of the gripper = 10.5cm,
Mass of the gripper link = 0.0705kg
Mass of the Base = 0.950kg

The torque of each servo motor at no load is obtained to be 10kgcm at 5V Dc input. This is needed to calculate the excess torque the motor has to develop in performing its required task. Moment of inertia is given as

$$M = arm\ weight \times ½\ arm\ length + motor\ weight\ x\ arm\ weight$$

At the gripper, the torque developed by the servo motor is 10.5 and the excess torque required is determined to be 9.62987 kg-cm

The torque needed at the wrist calculated to be 0.804125 kg-cm and the excess torque is 9.195875 kg-cm

At the elbow, the torque needed is determined to be 2.76556 kg-cm and the excess torque 7.23444 kg-cm
The torque at the shoulder is 3.12366 kg-cm and the excess torque is 6.87634 kg-cm

At the bottom which is the base, the torque required is 3.64666 kg-cm and the excess torque is 6.35334 kg-cm

The maximum torque that the mechanism developed at the gripper should be less than the torque at the base. For the mechanism, the maximum torque at the base is taken to be 5kg.cm giving allowance of 1.3177kg.cm. the radius of operation of the mechanism is the sum of all horizontal link of the mechanism given as 24.3cm.

V. MODELLING THE ARMATURE DC SERVO MOTORS FOR THE SYSTEM

The armature controlled dc servo motor is used extensively in the control system for its precision and stability characteristics [9]. The armature controlled dc motor modelling and its mathematical representation is as shown in Figure 5 and equations (9) to (17). It is assumed that the torque generated by the motor is proportional to the air-gap flux and also the armature current.

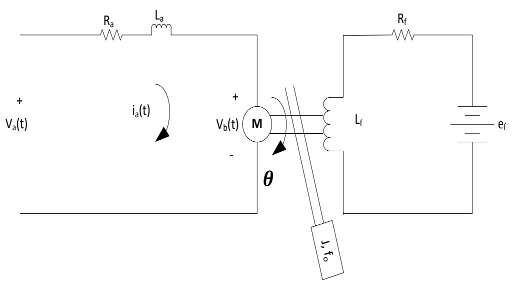

Fig. 5. The DC servo motor circuit diagram [9]

$i_a(t)$ is armature current (amperes)
R_a is armature resistance
$T_m(t)$ is motor torque (Nm)
K_i is Motor torque constant
L_a is armature inductance (Henries)
V_a *is* applied voltage (volts)
$W_m(t)$ is motor angular velocity (rad/sec)
K_e is motor voltage constant (v/rad/sec)
J_T is total inertia of motor armature plus load
α is acceleration (rad/sec^2)
θ_m *is* shaft angle in radians

The torque developed by the motor is given as

$$T_m(t)=K_T I_a(t) \quad (10)$$

Taking the friction force to be negligible, the back emf V_b is related to the angular velocity by

$$V_b = K_e W = K_e \frac{d\theta_m}{dt} \quad (11)$$

Applying Kirchhoff's voltage law around the electrical loop, we have

$$L_a \frac{di}{dt}+R_a i = \varepsilon_a K_e \frac{d\theta_m}{dt} \quad (12)$$

$$\varepsilon_a = i_a R_a+L_a \frac{di_a}{dt}+K_e W_m \quad (13)$$

Equation (14) is obtained after taking the Laplace transform of equation (13)

$$\varepsilon_a =(\frac{L_a}{R_a}s+1)R_a l_a+K_e W_m \quad (14)$$

Also it should be recalled that T=$K_T l_a$= $j_T\alpha$= $j_T W_m s$

$$l_a=\frac{T}{K_T}=\frac{j_T W_m s}{K_T} \quad (15)$$

Substitute eqn (15) into eqn (14)

$$\varepsilon_a - K_e W_M=(\frac{L_a}{R_a}s+1)R_a \frac{j_T W_m s}{K_T} \quad (16)$$

Hence, W_m becomes

$$\frac{(\varepsilon_a-K_e W_M)K_T}{(\frac{L_a}{R_a}s+1)\, R_a j_T s}=W_M \quad (17)$$

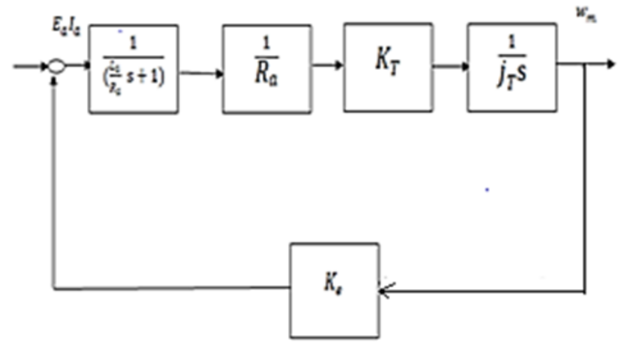

Fig. 6. The Block Diagram of the DC servomotor.

This closed loop transfer function of the armature dc controlled motor is obtained from the block diagram of Figure 6, equations (18) to (21).

$$\frac{W_m}{\varepsilon_a}=\frac{K_T}{R_a j_T s\left[\left(\frac{L_a}{R_a}\right)s+1\right]+K_e K_T} \quad (18)$$

$$\frac{W_m}{\varepsilon_a}=\frac{K_T}{(R_a j_T\frac{L_a}{R_a})S^2+j_T R_a S+K_e K_T} \quad (19)$$

$$\frac{W_m}{\varepsilon_a}=\frac{K_T}{(j_T L_a)S^2+j_T R_a S+K_e K_T} \quad (20)$$

$$\frac{\theta_m}{\varepsilon_a}=\frac{K_T}{(j_T L_a)S^3+j_T R_a S^2+K_e K_T} \quad (21)$$

For prototype design operation of the servo Dc motor, the following values are assumed for the servo motor parameters
R_a*(armature resistance)*=1.2Ω
L_a *(armature inductance)=0.07H*
$T_m(t)(motortorque) = 0.7(Nm)$

K_i*(Motor torque constant)=1N.m/A*
E_a (applied voltage) = 5 volts
w_m (t) (motor angular velocity) = 70RPM
K_e (motor voltage constant OR motor back – emf constant) = 0.01(v/rad/sec)
J_T (total inertia) = J_{motor} + J_{load}
a(angular acceleration) = (rad/sec^2
To calculate the angular acceleration ∝, is given as
∝ = 0.12217rad/sec^2
Therefore to calculate the J_{load} (moment of inertia of the load) = $\frac{T_{load}}{\propto}$. Now considering the motor at the gripper the torque derived at the previous section is 0.370125 kg.cm.
converting to Newton.neter : 0.370125× $\frac{9.81}{100}$
= 0.036309 N.m
Therefore $J_{load} = \frac{0.036309}{0.12217}$ = 0.2972 kg. m^2
For this servo dc motor J_m = 0.08 Kg.m^2

The $J_{Total} = J_m + J_{load}$

Therefore, that will yield;

$J_{Total} = 0.08 + 0.2972 = 0.3772$ kg.m

The transfer function for the first servo motor is therefore.

$$\frac{W_m}{\varepsilon_a} = \frac{1}{(0.3772*0.07)S^2+(0.3772*1.2)s+(1*0.01)}$$

$$\frac{W_m}{\varepsilon_a} = \frac{1}{(0.02640)S^2+0.45264s+0.01}$$

This is the transfer function for the servo motor at the gripper

At the wrist, torque derived earlier is used to calculate the total moment on inertia at the joint and the value is substituted into the general transfer function of a servo motor. For second motor at the wrist, the torque gotten is 0.74804 kg.cm, converting it to Newton.meter will give

$0.804125\text{x}\frac{9.81}{100} = 0.07888$Nm

Therefore$j_{load=}\frac{0.07888}{0.12217} = 0.6457\text{kg}.m^2$

For this servo motor $j_m = 0.05\text{kg}.m^2$

The $j_{total=}j_m + j_{load}$.Therefore that will yield;

$j_{total=}0.05 + 0.6457kg.m^2 = 0.6957\text{kg}.m^2$

The transfer function for the second servo motor is therefore:

$$\frac{W_m}{\varepsilon_a} = \frac{1}{(0.6957*0.07)S^2+(0.6957*1.2)s+0.01}$$

$$\frac{W_m}{\varepsilon_a} = \frac{1}{(0.04869)S^2+(0.8348)s+0.01}$$

This is the transfer function for the servo motor at the wrist

For third motor at the elbow, the torque gotten is 2.76556kg.cm, converting it to Newton.meter will give

$2.76556\ \text{x}\frac{9.81}{100} = 0.2713$Nm

Therefore $j_{load=}\frac{0.2713}{0.12217} = 2.22068\text{kg}.m^2$

For this servo motor $j_m = 0.05\text{kg}.m^2$

$j_{total=}j_m + j_{load}$. Therefore that will yield

$j_{total} = 0.05+2.22068\text{kg}.m^2 = 2.27068\text{kg}.m^2$

The transfer function for this third servo motor is therefore:

$$\frac{W_m}{\varepsilon_a} = \frac{1}{(2.27068*0.07)S^2+(2.27068*1.2)s+0.01} = \frac{1}{(0.158947)S^2+2.7248s+0.01}$$

This is the transfer function for the servo motor at the elbow

For the motor at the shoulder, the torque is $3.12366\text{kg}.m^2$,converting it to Newton.meter will give

$3.12366\text{x}\frac{9.81}{100} = 0.30643$Nm

Therefore $j_{load} = \frac{0.30643}{0.12217} = 2.5082\text{kg}.m^2$

For this servo dc motor $j_m = 0.05\text{kg}.m^2$.

The $j_{total=}j_m + j_{load}$.Therefore that will yield;

$j_{total=}0.05 + 2.5082\text{kg}.m^2 = 2.5582\text{kg}.m^2$

The transfer function for this fourth servo motor is therefore:

$$\frac{W_m}{\varepsilon_a} = \frac{1}{(2.5582*0.07)S^2+(2.5582*1.2)s+0.01}$$

$$= \frac{1}{(0.179074)S^2+3.06984s+0.01}$$

This is the transfer function for the servo motor at the shoulder The transfer function for this

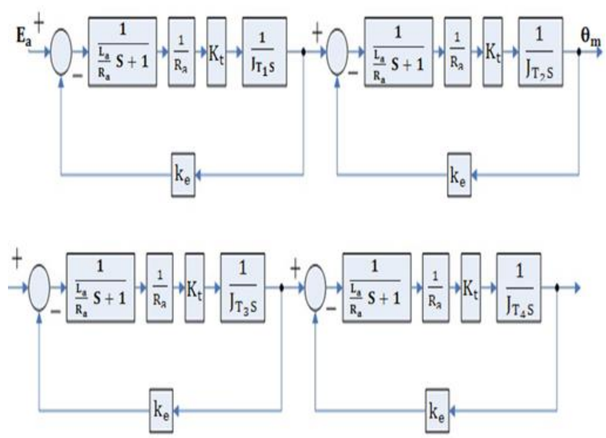

Fig. 7. Block diagram of the system

VI. SOFTWARE DEVELOPMENT

The electronic design for this mechanism at the transmitter involves the use of the two Arduino Atmega 283 microcontroller. It is an 8bit microcontroller and the first step involves configuring the register of the Arduino Atmega 283 to work with the desired pulse width modulation technique used.

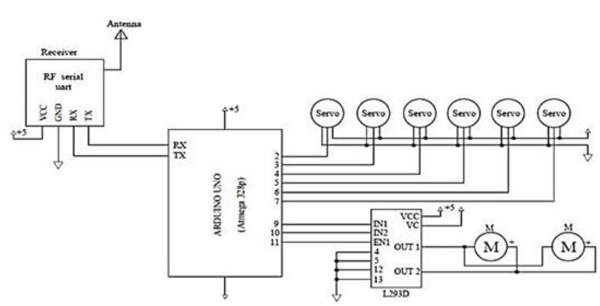

Fig. 8: Electrical design for the system

An external power supply is used to supply the servo motors and also the Arduino Atmega 283 microcontroller. The receiver is however connected to the arduino atmega 283 together with the servo motors. The two DC motors responsible for the movement of the two wheels of the mechanism is connected with the motor controller L293D and both are connected to the Arduino Atmega 283. The system is being powered by a rechargeable 8v battery.

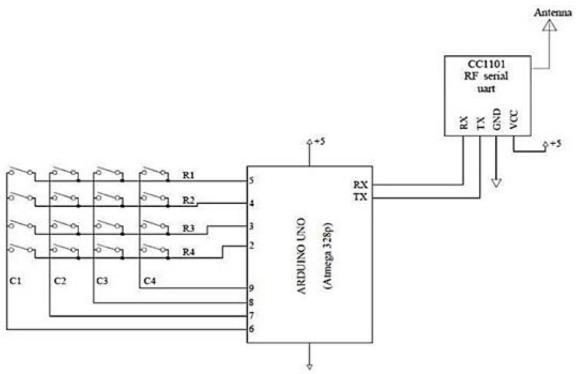

Fig. 9. Electrical design for the wireless RF remote control

Fig 8 shows the Arduino Atmega283 microcontroller connected with the transmitter. The dc battery of 5V rating is being connected with to power the controller. The push buttons also are arranged on the Vero board, thus connected to the microcontroller with cables.

VII. SYSTEM STABILITY

The transfer function for the whole model is gotten through the MatLab code below which brings about the test for system stability

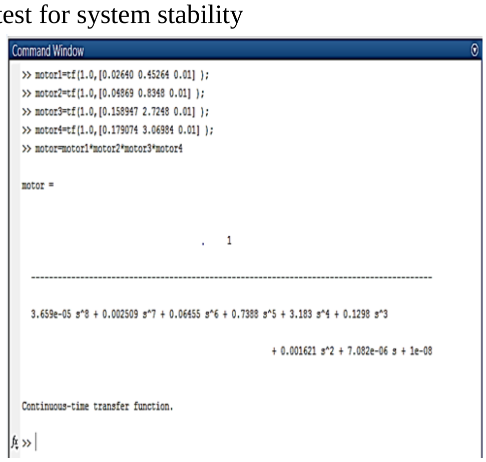

```
Command Window
>> motor1=tf(1.0,[0.02640 0.45264 0.01] );
>> motor2=tf(1.0,[0.04869 0.8348 0.01] );
>> motor3=tf(1.0,[0.158947 2.7248 0.01] );
>> motor4=tf(1.0,[0.179074 3.06984 0.01] );
>> motor=motor1*motor2*motor3*motor4

motor =

                                  1
  -----------------------------------------------------------------------------------
  3.659e-05 s^8 + 0.002509 s^7 + 0.06455 s^6 + 0.7388 s^5 + 3.183 s^4 + 0.1298 s^3

                                         + 0.001621 s^2 + 7.082e-06 s + 1e-08

Continuous-time transfer function.

>>
```

Fig...10. MatLab code for acquiring the transfer function.

The system yields the transfer function below:

$$= \frac{1}{3.659e^{-5}s^8+0.002509s^7+0.06455s^6+0.7388s^5+3.183s^4+0.1298s^3+0.001621s^2+7.082e^{-6}s+1e^{-8}}$$

VIII. RESULTS AND DISCUSSION

The matrices in fig 11 were generated for the state space form.

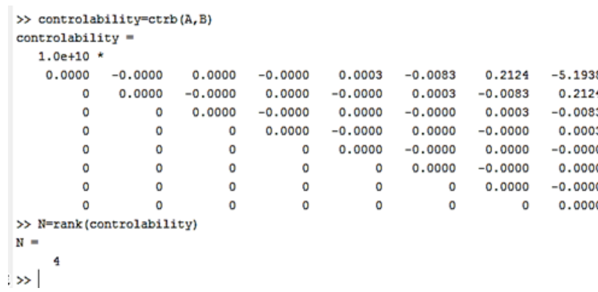

```
>> controlability=ctrb(A,B)
controlability =
   1.0e+10 *
    0.0000   -0.0000    0.0000   -0.0000    0.0003   -0.0083    0.2124   -5.1938
         0    0.0000   -0.0000    0.0000   -0.0000    0.0003   -0.0083    0.2124
         0         0    0.0000   -0.0000    0.0000   -0.0000    0.0003   -0.0083
         0         0         0    0.0000   -0.0000    0.0000   -0.0000    0.0003
         0         0         0         0    0.0000   -0.0000    0.0000   -0.0000
         0         0         0         0         0    0.0000   -0.0000    0.0000
         0         0         0         0         0         0    0.0000   -0.0000
         0         0         0         0         0         0         0    0.0000
>> N=rank(controlability)
N =
     4
>>
```

Fig. 11. The controllability matrix and the rank of matrix

Fig 12 shows the rank of the controllability matrix is not full. A full rank is when the value of the rank is equal to the value of the row or column of a square matrix (i.e a n x n matrix having a rank of n). The controllable matrix for this mechanism is an 8 x 8 matrix and the rank is 4 meaning the rank is not full hence it is not controllable.

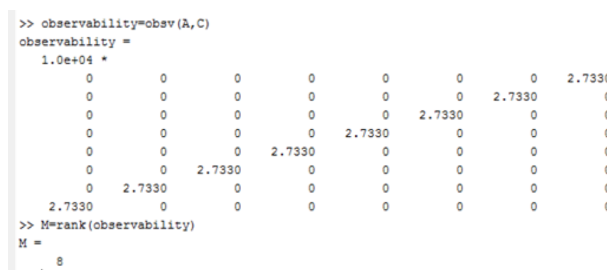

```
>> observability=obsv(A,C)
observability =
   1.0e+04 *
         0         0         0         0         0         0         0    2.7330
         0         0         0         0         0         0    2.7330         0
         0         0         0         0         0    2.7330         0         0
         0         0         0         0    2.7330         0         0         0
         0         0         0    2.7330         0         0         0         0
         0         0    2.7330         0         0         0         0         0
         0    2.7330         0         0         0         0         0         0
    2.7330         0         0         0         0         0         0         0
>> M=rank(observability)
M =
     8
```

Fig. 12. The observability matrix and the rank of matrix

Fig 12 shows that the rank of the observability matrix is full. A full rank is when the value of the rank is equal to the value of the row or column of the square matrix (i.e a n x n matrix having a rank of n). The observability matrix for this system is an 8 x 8 matrix and the rank is full hence it is controllable.

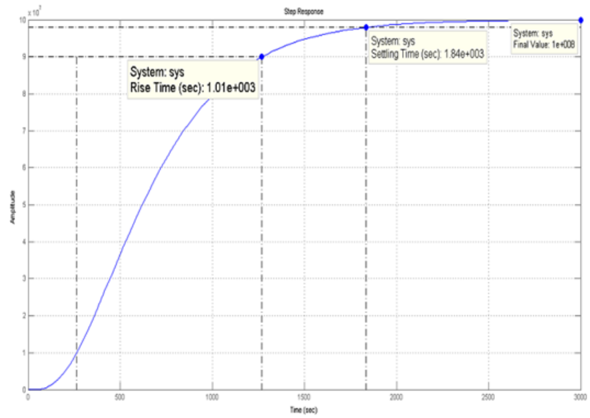

Fig. 13. The step response plot showing the value of the step information

Fig 13 shows the step response of the transfer function of the system is displayed. The rise time of the system is 1.01e + 03secs and the settling time is 1.84e + 03secs. The system steady state is at 1e + 08secs. This is considered good for the system.

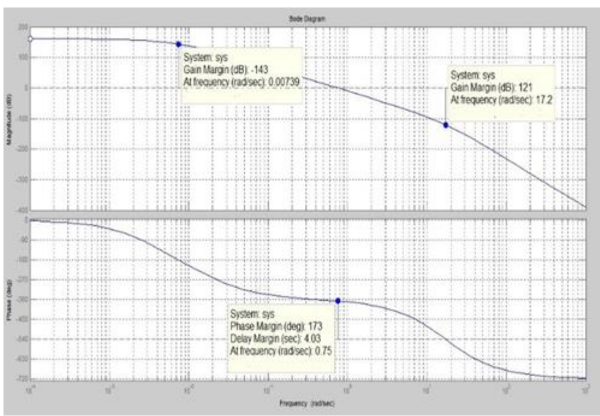

Fig. 14. The bode plot for the system.

The plot illustrates that the system has a phase margin of 173^0 at a gain cross frequency of 0.75rad/secs. The point on the magnitude plot in which the curve crosses 0*dB* is traced down in the phase plot and that the corresponding point on the phase plot is the phase margin. Consequently, for the gain margin, the point on the phase plot that the curve crosses -180^0 is traced up to the magnitude plot and corresponding point on the magnitude plot curve is the gain margin. On this plot the phase plot did crosses the -180^0 at the phase crossover frequency of 0.75 rad/secs, the gain margin at this point is -143dB

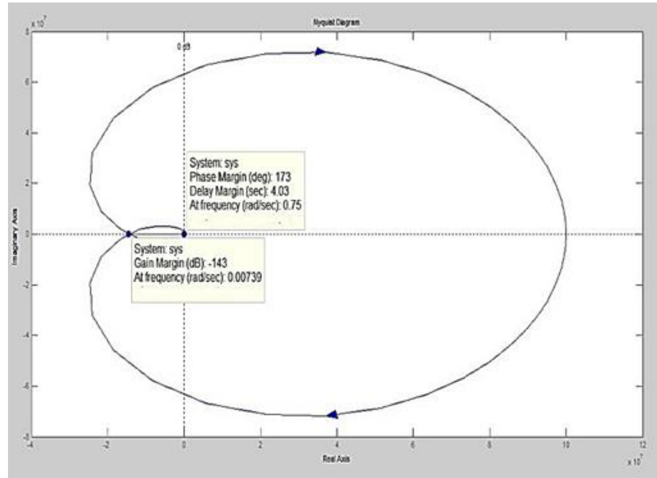

Fig. 15. The polar plot for the system.

The polar plot shows that the phase Margin gotten from the bode plot is 121^0. The gain Margin of the polar plot is also the same as that of the bode plot and it is -143^0. This shows that the system is stable.

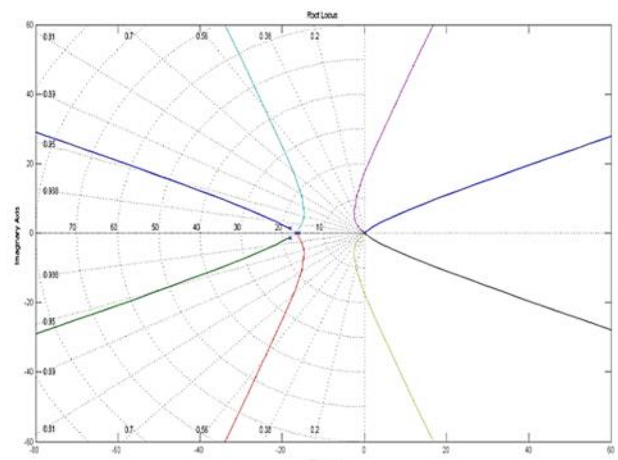

Fig. 16. The Root locus plot of the System.

Fig 16 shows that the root locus has its zeros on the left hand side of the plot, this implies that the system is more stable and its speed up the settling time of the system response.

A. Establishing the Robustness with Reference Tracking

Fig 17 shows the initial step plot of the system, the response time is 544.5 seconds our system is stable and the robustness is 0.6. The rise time 276 seconds and the settling time is 2210 seconds.

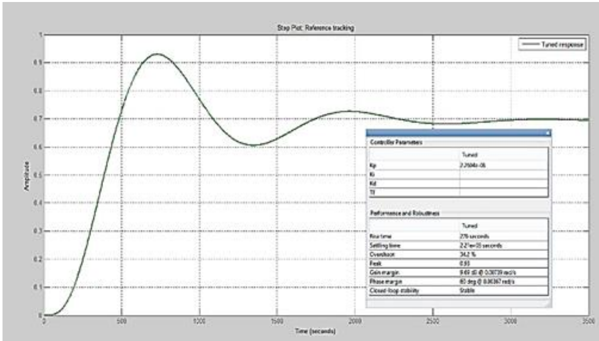

Fig. 17. Initial System response graph

The system is stable but the rise time is too high. PID controller is introduced to tune the system to reduce the rising time and also increase the robustness of the system.

From Fig 18 the response time is increased the 126 seconds and the robustness of the plant is 0.84seconds. The rise time was reduced from 276 seconds to 66.1 seconds and the system is stable. Also, the settling time has reduced. The system is stable and has a robustness of 0.84. this shows that with the aid of the PID controller the system is more stable and its rise time is faster than before and it has good robustness and performance.

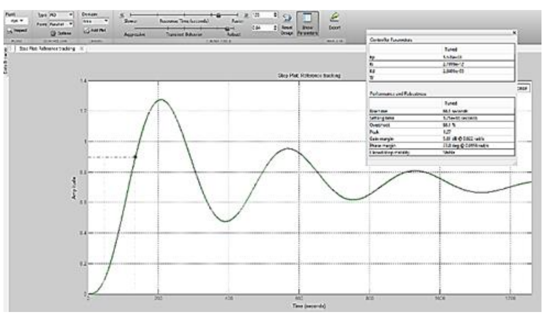

Fig 18. Final system response graph

IX. CONCLUSION

The assistive device will be able to meet most of the challenges of impaired people in society. The device was designed to fulfil the required tasks without the impaired facing any hindrances due to the lack of muscle activity. The Robotic Arm designed is unique to impaired people specific conditions of Athetoid Quadriplegia. As a result, the controllers of this device are constructed to ease the usage. Assistive robots will help people with impaired arm functions perform ordinary tasks, like eating and drinking, or opening a desk drawer.

The assistive robot construction breakdown involves the use of a microcontroller and the C – Programming language for programming, the radio frequency transmitter, and the receiver together with the servo motor controls. This device will provide the impaired an opportunity to partake in the simple everyday tasks.

REFERENCES

[1] Zunt, Dominik. "Who did actually invent the word "robot" and what does it mean?". The Karel Čapek website. Retrieved 09-11- 2011.

[2] Nikku, S., “Introduction to Robotics” USA: John Wiley & Sons, 2011.

[3] Nehmzow, U., ”Mobile Robotics: a practical introduction”, UK: Springer, 05-04-2003.

[4] Muir, F. P., Neuman, P. C., "Pulsewidth Modulation Control of Brushless DC Motors for Robotic Applications", IEEE Transactions on Industrial Electronics, Issue 3, Vol. 32, pp.222-229, 1985.

[5] Lin, I. H., Liu, C. Y., Chen, L. C., "Evaluation of Human-Robot Arm Movement Imitation", Proceedings of 8th Asian Control Conference (ASCC), pp.287-292, 2011.

[6] Craig, j.j (2005). The mechanics and control of mechanical manipulators. Direction of freedom (DOF): Pearson Education International. pp.333-357, 2012

[7] Nones, Y. A., “Heterogeneous Modelling & Design of a Robot Arm Control System”, Illinois Tech Robotics (ITR), pp.1-6, 2003.

[8] Park, I. D., Park, C., Do, H., Choi, T., Kyung, J., Design and Analysis of Dual Arm Robot Using Dynamic Simulation" IEEE 10th International Conference on Ubiquitous Robots and Ambient Intelligence (URAI), pp. 681-682, 2013.

[9] RobotWiki. (2014, September 23). Servos. Retrieved November 5, from psurobotic http://www.psurobotics.org/wiki/index.php?title=servos

[10] Scott Schaut (2006). Robots of Westinghouse: 1924-Today. Mansfield Memorial Museum. ISBN 0-9785844-1-4. Received 09-11- 2010

[11] Bo Li (2013), Rotational Double Inverted Pendulum, M.Sc. Thesis, School of Engineering, University of Dayton, Dayton, Ohio, U.S.

[12] Ranwaka, R., Perera, T. R., Adhuran, J., Samarakoon, C., & Rajakaruna, R. (2013), 111-Microcontroller Based Robot Arm with Three – Dimensional Reach.